



CERN-EP-2022-040

11 March 2022

First measurement of antideuteron number fluctuations at energies available at the Large Hadron Collider

ALICE Collaboration

Abstract

The first measurement of event-by-event antideuteron number fluctuations in high energy heavy-ion collisions is presented. The measurements are carried out at midrapidity ($|\eta| < 0.8$) as a function of collision centrality in Pb–Pb collisions at $\sqrt{s_{NN}} = 5.02$ TeV using the ALICE detector. A significant negative correlation between the produced antiprotons and antideuterons is observed in all collision centralities. The results are compared with coalescence calculations, which fail to describe the measurement, in particular if a correlated production of protons and neutrons is assumed. Thermal-statistical model calculations describe the data within uncertainties only for correlation volumes that are different with respect to those describing proton yields and a similar measurement of net-proton number fluctuations.

arXiv:2204.10166v1 [nucl-ex] 21 Apr 2022

The production of nuclei and antinuclei in heavy-ion collisions has been extensively studied in the last two decades. Nevertheless, this wealth of results is still not able to clarify the mechanism behind nuclei and antinuclei formation in heavy-ion collisions. Indeed, the two best fitting models, the coalescence [1–3] and the statistical hadronisation models (SHM) [4, 5], give very similar predictions for the production rates of nuclei and antinuclei in heavy-ion collisions. This similarity calls for new observables to decisively discriminate between these two approaches.

The SHM describes the system as a hadron-resonance gas in thermal equilibrium at hadron emission, hence it predicts particle yields starting from the volume (V) and the temperature of the system at chemical freeze-out (T_{chem}). The Grand Canonical Ensemble (GCE) formulation of the SHM fits the measured production yields of light hadrons and nuclei in central Pb–Pb collisions at center-of-mass energy ($\sqrt{s_{\text{NN}}}$) of 2.76 TeV with $T_{\text{chem}} = 156.5$ MeV [6]. The coalescence model uses a different approach to explain the production of nuclei: the size of the nucleon-emitting source, accessible through the analysis of femtoscopic correlations [7], the momentum distribution of the nucleons, as well as the nuclear wave function, are inputs that determine the formation probability of bound states [3, 8]. While using statistical hadronisation it is possible to compute directly the absolute yields of particles, in the hadron coalescence model the yield of bound states can be computed only relative to the production of its components and as a function of system size.

In a recent model study [9], it is shown that the higher order cumulants of the deuteron yield distribution and correlation between proton (p) and deuteron (d) production can be used to distinguish between coalescence and SHM. Higher order cumulants κ_m of the multiplicity distribution for $m < 4$ and the Pearson correlation coefficient (ρ_{ab}) between different identified particles a and b can be expressed as

$$\kappa_1 = \langle n \rangle, \quad (1)$$

$$\kappa_m = \langle (n - \langle n \rangle)^m \rangle, \quad (2)$$

$$\rho_{\text{ab}} = \langle (n_a - \langle n_a \rangle)(n_b - \langle n_b \rangle) \rangle / \sqrt{\kappa_{2a} \kappa_{2b}}, \quad (3)$$

where n , $\langle n \rangle$, and m are the event-by-event particle numbers, event average of particle numbers and order of the cumulants, respectively. The $\langle n_a \rangle$ ($\langle n_b \rangle$) and κ_{2a} (κ_{2b}) are the first and second order cumulants of the multiplicity distribution of particle a (b). In the GCE formulation of the SHM, the event-by-event deuteron multiplicity distribution is expected to follow the Poisson distribution [10]. Therefore various ratios between cumulants of different order of the deuteron multiplicity distribution such as κ_2/κ_1 , κ_3/κ_2 are equal to unity in the GCE SHM. In a simple coalescence scenario, if deuterons are produced by the coalescence of thermally produced protons and neutrons, then the event-by-event deuteron distribution is expected to deviate from the Poisson baseline [9]. By definition, the coalescence model also introduces a negative correlation between the measured proton and deuteron numbers in absence of any initial correlation between proton and neutron. On the other hand, one does not expect any correlation between the measured p and d in the GCE SHM as the baryon productions from a thermal source are independent from each other. However, in the Canonical Ensemble (CE) formulation of the SHM, particle production is constrained by the conservation of the net baryon numbers on an event-by-event basis, which can also introduce a negative correlation between measured proton and deuteron in SHM and a deviation of cumulant ratios from the Poisson baseline [10, 11].

In this letter, the first measurements of the κ_2/κ_1 ratio of antideuteron (antiparticles are used throughout the analysis to reject the contamination from secondary deuterons coming from spallation processes in the beam pipe) multiplicity distribution and correlation ($\rho_{\bar{p}\bar{d}}$) between measured antideuterons (\bar{d}) and antiprotons (\bar{p}) are presented. Measurements are compared with predictions from the SHM and coalescence model in order to shed light on the deuteron synthesis mechanism. The results presented in this letter are obtained using data collected during the 2015 Pb–Pb LHC run at $\sqrt{s_{\text{NN}}} = 5.02$ TeV.

The ALICE detector and its performance are described in detail in Refs. [12, 13]. Collision events are selected by using the information from the V0C and V0A scintillator arrays [14], located on both

sides of the interaction point, covering the pseudorapidity intervals $-3.7 < \eta < -1.6$ and $2.8 < \eta < 5.1$, respectively. Events are selected with a minimum-bias (MB) trigger which requires at least one hit in both the V0A and the V0C detectors. In addition, only events with the primary vertex position within 10 cm along the beam axis to the nominal interaction point are selected to benefit from the full acceptance of the detector. Furthermore, to ensure the best possible performance of the detector and proper normalisation of the results, events with more than one reconstructed primary interaction vertex (pile-up events) are rejected. In total, about 100 million MB events are selected for analysis. Furthermore, the selected events are divided into centrality classes based on the measured amplitude distribution in the V0A and V0C counters as described in Ref. [15]. Central Pb–Pb collisions (head-on collisions) are obtained from the top 10% of the amplitude distribution corresponding to hadronic interactions and peripheral Pb–Pb collisions are obtained from the 70–80% region of the same distribution.

The charged-particle tracks are reconstructed in the ALICE central barrel with the Inner Tracking System (ITS) [13] and the Time Projection Chamber (TPC) [16], which are located within a solenoid that provides a homogeneous magnetic field of up to 0.5 T in the direction of the beam axis. These two subsystems provide full azimuthal coverage for charged-particle trajectories in the pseudorapidity interval $|\eta| < 0.8$. The transverse momentum range is restricted to $0.4 < p_T < 1.8$ GeV/c to select the \bar{p} and \bar{d} with high purity. Moreover, to guarantee a track-momentum resolution of 2% in the relevant p_T range and an energy loss (dE/dx) resolution in the TPC of 5%, the selected tracks are required to have at least 70 out of a maximum possible 159 reconstructed space points in the TPC, and at least one hit in the two innermost layers of the ITS. This selection also assures a resolution better than 300 μm [13] on the distance of the closest approach to the primary vertex in the plane perpendicular (DCA_{xy}) and parallel (DCA_z) to the beam axis for the selected tracks. In addition, the χ^2 per space point in the TPC and the ITS from the track fit are required to be less than 4 and 36, respectively. Daughter tracks from reconstructed secondary weak-decay kink topologies were rejected and a suppression of the weak-decay particles are obtained by selecting tracks with $|DCA_z|$ and $|DCA_{xy}|$ less than 1.0 and 0.1 cm, respectively.

The \bar{d} and \bar{p} are identified via the specific energy loss dE/dx in the gas volume of the TPC and the flight time of a particle from the primary vertex of the collision to the Time-of-Flight (TOF) detector. The $n(\sigma_i^{\text{TPC}})$ variable represents the particle identification (PID) response in the TPC expressed in terms of the deviation between the measured and the expected dE/dx for a particle species i , normalized by the detector resolution σ . The expected dE/dx is computed with a parameterised Bethe–Bloch function [13]. The \bar{p} and \bar{d} are identified using $-2 < |n(\sigma_i^{\text{TPC}})| < 4$ in the range $0.4 < p_T < 0.6$ GeV/c and $0.8 < p_T < 1.0$ GeV/c, respectively. Particle identification on a track-by-track basis using the TPC is limited to low momenta. Therefore, to identify \bar{d} (\bar{p}) in the range $1.0 < p_T < 1.8$ GeV/c ($0.6 < p_T < 0.9$ GeV/c), an additional selection of $3.0 < m^2 < 4.2$ GeV²/c⁴ ($0.6 < m^2 < 1.2$ GeV²/c⁴) using the Time-of-Flight (TOF) [17] detector is applied, where the square of the particle mass, m^2 , is obtained by combining the information of the flight time with the trajectory length of the particle. The selection of \bar{d} is restricted to the range $0.8 < p_T < 1.8$ GeV/c in order to keep the overall \bar{d} purity above 90%. The \bar{p} selection is restricted to exactly half of the p_T range of \bar{d} according to the coalescence mechanism. This selection results in a purity of the selected \bar{p} sample above 95%. The impurity in \bar{d} selection can lead to an autocorrelation with the selected \bar{p} and affect the $\rho_{\bar{p}\bar{d}}$. The effect is negligible in our measurement as the \bar{d} and \bar{p} are mostly selected in a separated acceptance and in the common p_T interval the \bar{d} purity is $\sim 99\%$. Selected \bar{d} and \bar{p} numbers in each event are further used to obtain the higher order cumulants and correlation.

Measured cumulants are corrected for the \bar{d} and \bar{p} reconstruction efficiencies and their event-by-event fluctuations assuming a binomial response of the detectors. The binomial-based method of efficiency correction [18] is a two-step method. First, the efficiency of \bar{d} and \bar{p} reconstruction in the ALICE detector is obtained using a simulation based on GEANT4, which correctly describes the interaction of \bar{p} and \bar{d} with the material of the detectors [19]. Then, the cumulants and correlation coefficient are corrected for

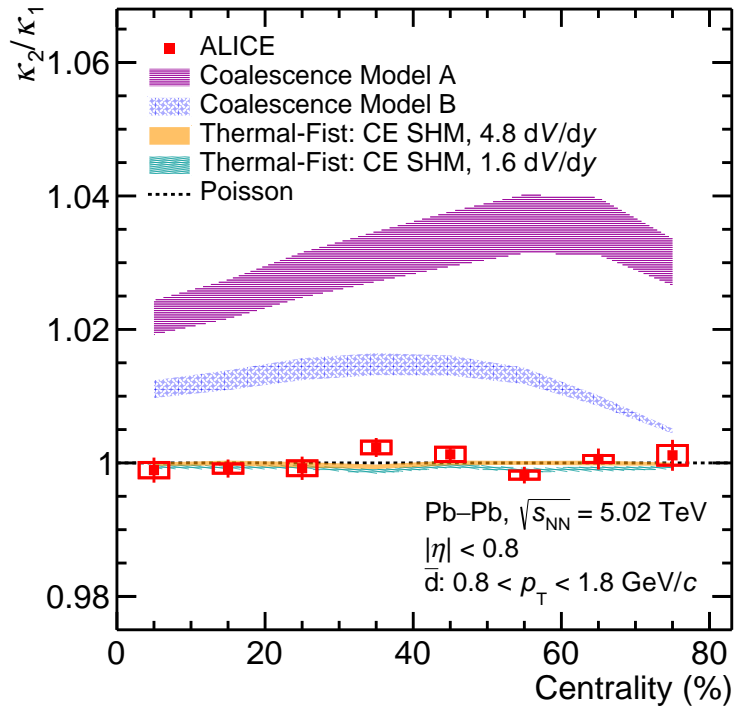


Figure 1: Second order to first order cumulant ratio of the \bar{d} multiplicity distribution as a function of collision centrality in Pb–Pb collisions at $\sqrt{s_{NN}} = 5.02$ TeV. Statistical and systematic uncertainties are shown by the bars and boxes, respectively. Measured cumulant ratios are compared with estimations from the CE version of the SHM for two different baryon number conservation volumes and from a simple coalescence model. The width of the SHM model bands corresponds to the statistical uncertainty of the model estimation, whereas the width of the band for coalescence model corresponds to the uncertainty coming from the variation of the coalescence parameters.

the reconstruction efficiencies and their fluctuations using analytic expressions as discussed in Ref. [18]. Typical values of \bar{p} and \bar{d} reconstruction efficiencies for the studied p_T ranges in the TPC and TOF are about 70% and 25%, respectively. The efficiency-corrected cumulants and correlation are further corrected for the centrality bin width effect [20] to suppress the initial volume fluctuations which arise from the initial state (size and shape) fluctuations.

The statistical uncertainties on the efficiency corrected κ_2/κ_1 ratio and $\rho_{\bar{p}\bar{d}}$ are obtained by the subsample method [21]. The systematic uncertainties on the observables are estimated by varying the track selection and PID criteria. The systematic uncertainties due to track selection include the variation of the selection criteria on DCA_{xy} , DCA_z , the number of reconstructed space points in the TPC, and the quality of the track fit from their nominal values. The systematic uncertainties due to PID are calculated by varying the default $n(\sigma^{TPCi})$ and m^2 criteria. Systematic uncertainties due to each of these sources are considered as uncorrelated and the total systematic uncertainty on the observables is obtained by adding all the contributions in quadrature.

The resulting ratio of the second to first order cumulant for \bar{d} is shown in Fig. 1 for different centrality classes. The data is found to be consistent with unity within uncertainties as expected from a Poisson distribution and does not exhibit a significant centrality dependence. Measurements are also compared with estimations from the CE version of the SHM for two different correlation volumes (V_c) for baryon number conservation, $V_c = 4.8$ dV/dy (orange band in figures) and $V_c = 1.6$ dV/dy (green band in figures). The choice of two different V_c is discussed below. In the SHM model the temperature is fixed to $T = 155$ MeV [5], the volume fitted to the published pion, kaon, and proton yields at midrapidity [22], and the net-baryon number set to 0. Measurements are found to be consistent with the SHM model for both of the V_c . In contrast to the corresponding ratio for p and \bar{p} [23, 24], no strong dependence on the V_c

is seen due to the fact that only a small fraction of the total antibaryon number is carried by \bar{d} [10, 25]. Remarkably, the data differs from the calculations of the coalescence model, which predicts a deviation larger than 1% from the Poisson baseline as explained in Ref. [9]. Two shaded bands are shown for the coalescence model: the red one assumes full correlation among protons and neutrons produced in the collision (Model A), while the blue one assumes completely independent proton and neutron production fluctuations (Model B).

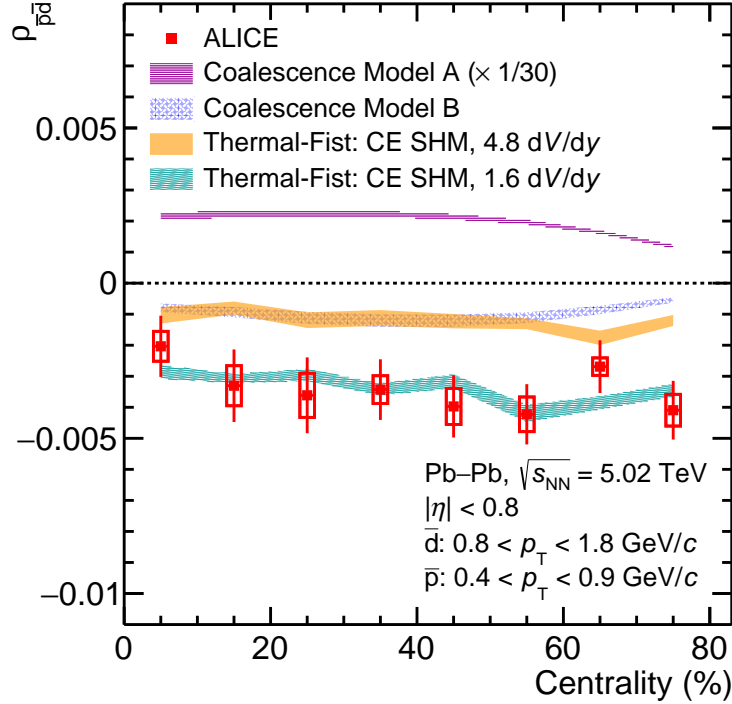


Figure 2: Pearson correlation between the measured \bar{p} and \bar{d} as a function of collision centrality in Pb-Pb collisions at $\sqrt{s_{NN}} = 5.02$ TeV. Bars and boxes represent statistical and systematic uncertainties, respectively. Measured correlations are compared with estimations from the CE version of the SHM for two different baryon number conservation volumes and from a simple coalescence model.

Figure 2 shows $\rho_{\bar{p}\bar{d}}$ as a function of the collision centrality. A small negative correlation of $O(0.1\%)$ is observed, i.e. in events with at least one \bar{d} , there are $O(0.1\%)$ less \bar{p} observed than in an average event. The negative correlation observed in data is expected in the coalescence model (shown by the blue band in Fig. 2) where \bar{p} and \bar{n} from two independent sources coalesce to produce \bar{d} . It has to be noted that models based on fully correlated proton and neutron fluctuations (Model A in Ref. [9]) predict values of ρ around 6% and are ruled out by data. On the other hand, the measured negative correlation between \bar{p} and \bar{d} is also expected by the CE version of the SHM which introduces a negative correlation between \bar{p} and \bar{d} through the conservation of a fixed net-baryon number. The predicted correlation in the SHM increases with decreasing correlation volume V_c for baryon number conservation which is used in the following for a determination of V_c . In order to determine the correlation volume for the baryon quantum number, a χ^2 minimization is performed by varying the V_c parameter in the SHM model and comparing the result to the measured correlation as a function of centrality. The V_c interval probed in this case spans from 1 to 5 units of rapidity, and the value that describes best the measurement is $V_c = 1.6 \pm 0.3$ dV/dy with a fit probability of 85%. The SHM configuration with $V_c = 4.8$ dV/dy that correctly describes the net-proton number fluctuations in central Pb-Pb collisions [25, 26] is compatible within uncertainties with the measured $\rho_{\bar{p}\bar{d}}$ only in central collisions. Conversely, this configuration is excluded with a 4σ confidence level when compared with the measurements in all centrality classes.

Several consistency checks such as the correlation between \bar{p} and \bar{d} from different events, the correlation

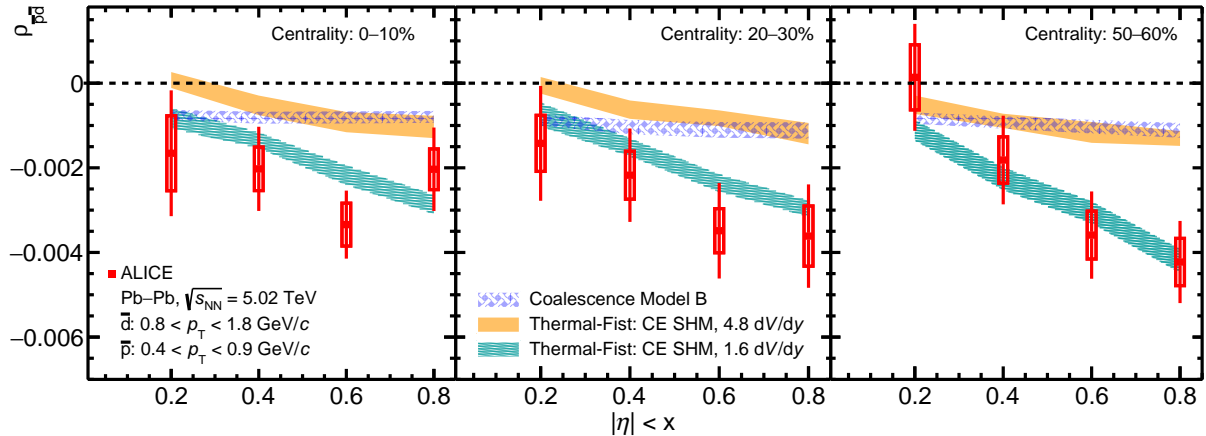


Figure 3: Dependence of \bar{p} - \bar{d} correlation on pseudorapidity acceptance of \bar{p} and \bar{d} selection in Pb-Pb collisions at $\sqrt{s_{NN}} = 5.02$ TeV for three different centrality classes. Measurements are compared with calculations from the CE version of the SHM and coalescence model.

between antibaryon (\bar{d}) and baryon (p) were performed for a better understanding of the observed correlation. The correlation between \bar{p} and \bar{d} from mixed events is consistent with zero as expected. However, a positive correlation is observed between antibaryon and baryon. This positive correlation is expected due to baryon number conservation [10], whereas in simple coalescence model no correlation between baryon and antibaryon is expected as \bar{d} is not produced from the coalescence of p .

Figure 3 shows the same Pearson correlation coefficient in three centrality intervals as a function of the η acceptance of \bar{p} and \bar{d} selection. The observed anticorrelation is increasing with acceptance, and the effect is more pronounced for peripheral collisions. Simple coalescence calculations do not capture this trend. On the other hand, this measurement should motivate further calculations with more refined coalescence models. The same decreasing trend is seen in the SHM with $V_c = 1.6$ dV/dy. In the CE version of SHM model, anticorrelation between antibaryons depends on the fraction of antibaryon number in the acceptance out of the total conserved antibaryon numbers [10, 11, 24, 26]. Therefore, the increase of $\rho_{\bar{p}\bar{d}}$ with increasing acceptance can be understood as a consequence of baryon number conservation.

In summary, the measurement of \bar{d} production fluctuation is a valuable tool to challenge the nucleosynthesis models used for hadronic collisions. Simple coalescence models fail to fit simultaneously the measurement of the cumulants ratios and the correlation coefficient $\rho_{\bar{p}\bar{d}}$. The coalescence model shows a great sensitivity to the initial correlation between the proton and the neutron production, hence further theoretical developments might improve the comparison with the measurement. In recent studies, state-of-the-art CE SHM models are describing simultaneously proton yields and net-proton fluctuation measurements finding large $V_c \approx 3-5$ dV/dy [25–27]. Surprisingly, deuteron production measurements [5] as well as the fluctuation measurements presented here indicate a significantly smaller correlation volume for the baryon number. Under the assumption that V_c is independent of collision centrality, the value $V_c = 1.6 \pm 0.3$ dV/dy is obtained. More sophisticated approaches including partial chemical equilibrium [28] or implementation of the interaction of hadrons through phase-shift [29, 30] could help in resolving this conundrum. The results of this paper present a severe challenge to the current understanding of nuclei production in heavy-ion collisions at the LHC energies.

References

- [1] S. Mrowczynski, “Deuteron formation mechanism”, *J. Phys. G* **13** no. 9, (1987) 1089–1097.
- [2] R. Scheibl and U. W. Heinz, “Coalescence and flow in ultrarelativistic heavy ion collisions”, *Phys.*

- Rev. C* **59** (1999) 1585–1602, arXiv:nuc1-th/9809092.
- [3] K.-J. Sun, C. M. Ko, and B. Dönigus, “Suppression of light nuclei production in collisions of small systems at the Large Hadron Collider”, *Phys. Lett. B* **792** (2019) 132–137, arXiv:1812.05175 [nucl-th].
- [4] A. Andronic, P. Braun-Munzinger, J. Stachel, and H. Stoecker, “Production of light nuclei, hypernuclei and their antiparticles in relativistic nuclear collisions”, *Phys. Lett. B* **697** (2011) 203–207, arXiv:1010.2995 [nucl-th].
- [5] V. Vovchenko, B. Dönigus, and H. Stoecker, “Multiplicity dependence of light nuclei production at LHC energies in the canonical statistical model”, *Phys. Lett. B* **785** (2018) 171–174, arXiv:1808.05245 [hep-ph].
- [6] A. Andronic, P. Braun-Munzinger, K. Redlich, and J. Stachel, “Decoding the phase structure of QCD via particle production at high energy”, *Nature* **561** no. 7723, (2018) 321–330, arXiv:1710.09425 [nucl-th].
- [7] **ALICE** Collaboration, S. Acharya *et al.*, “Search for a common baryon source in high-multiplicity pp collisions at the LHC”, *Phys. Lett. B* **811** (2020) 135849, arXiv:2004.08018 [nucl-ex].
- [8] K. Blum, K. C. Y. Ng, R. Sato, and M. Takimoto, “Cosmic rays, antihelium, and an old navy spotlight”, *Phys. Rev. D* **96** no. 10, (2017) 103021, arXiv:1704.05431 [astro-ph.HE].
- [9] Z. Fecková, J. Steinheimer, B. Tomášik, and M. Bleicher, “Formation of deuterons by coalescence: Consequences for deuteron number fluctuations”, *Phys. Rev. C* **93** no. 5, (2016) 054906, arXiv:1603.05854 [nucl-th].
- [10] P. Braun-Munzinger, B. Friman, K. Redlich, A. Rustamov, and J. Stachel, “Relativistic nuclear collisions: Establishing a non-critical baseline for fluctuation measurements”, *Nucl. Phys. A* **1008** (2021) 122141, arXiv:2007.02463 [nucl-th].
- [11] M. Borej and A. Bzdak, “Factorial cumulants from global baryon number conservation”, *Phys. Rev. C* **102** no. 6, (2020) 064908, arXiv:2006.02836 [nucl-th].
- [12] **ALICE** Collaboration, K. Aamodt *et al.*, “The ALICE experiment at the CERN LHC”, *JINST* **3** (2008) S08002.
- [13] **ALICE** Collaboration, B. B. Abelev *et al.*, “Performance of the ALICE Experiment at the CERN LHC”, *Int. J. Mod. Phys. A* **29** (2014) 1430044, arXiv:1402.4476 [nucl-ex].
- [14] **ALICE** Collaboration, E. Abbas *et al.*, “Performance of the ALICE VZERO system”, *JINST* **8** (2013) P10016, arXiv:1306.3130 [nucl-ex].
- [15] **ALICE** Collaboration, B. Abelev *et al.*, “Centrality determination of Pb-Pb collisions at $\sqrt{s_{NN}} = 2.76$ TeV with ALICE”, *Phys. Rev. C* **88** no. 4, (2013) 044909, arXiv:1301.4361 [nucl-ex].
- [16] J. Alme *et al.*, “The ALICE TPC, a large 3-dimensional tracking device with fast readout for ultra-high multiplicity events”, *Nucl. Instrum. Meth. A* **622** (2010) 316–367, arXiv:1001.1950 [physics.ins-det].
- [17] A. Akindinov *et al.*, “Performance of the ALICE Time-Of-Flight detector at the LHC”, *Eur. Phys. J. Plus* **128** (2013) 44.
- [18] T. Nonaka, M. Kitazawa, and S. Esumi, “More efficient formulas for efficiency correction of cumulants and effect of using averaged efficiency”, *Phys. Rev. C* **95** no. 6, (2017) 064912, arXiv:1702.07106 [physics.data-an]. [Erratum: Phys.Rev.C 103, 029901 (2021)].

- [19] **ALICE** Collaboration, S. Acharya *et al.*, “Measurement of the low-energy antideuteron inelastic cross section”, *Phys. Rev. Lett.* **125** no. 16, (2020) 162001, arXiv:2005.11122 [nucl-ex].
- [20] X. Luo, J. Xu, B. Mohanty, and N. Xu, “Volume fluctuation and auto-correlation effects in the moment analysis of net-proton multiplicity distributions in heavy-ion collisions”, *J. Phys. G* **40** (2013) 105104, arXiv:1302.2332 [nucl-ex].
- [21] **ALICE** Collaboration, S. Acharya *et al.*, “Relative particle yield fluctuations in Pb-Pb collisions at $\sqrt{s_{NN}} = 2.76$ TeV”, *Eur. Phys. J. C* **79** no. 3, (2019) 236, arXiv:1712.07929 [nucl-ex].
- [22] **ALICE** Collaboration, S. Acharya *et al.*, “Production of charged pions, kaons, and (anti-)protons in Pb-Pb and inelastic *pp* collisions at $\sqrt{s_{NN}} = 5.02$ TeV”, *Phys. Rev. C* **101** no. 4, (2020) 044907, arXiv:1910.07678 [nucl-ex].
- [23] **STAR** Collaboration, M. Abdallah *et al.*, “Cumulants and correlation functions of net-proton, proton, and antiproton multiplicity distributions in Au+Au collisions at energies available at the BNL Relativistic Heavy Ion Collider”, *Phys. Rev. C* **104** no. 2, (2021) 024902, arXiv:2101.12413 [nucl-ex].
- [24] V. Vovchenko, V. Koch, and C. Shen, “Proton number cumulants and correlation functions in Au-Au collisions at $s_{NN}=7.7-200$ GeV from hydrodynamics”, *Phys. Rev. C* **105** no. 1, (2022) 014904, arXiv:2107.00163 [hep-ph].
- [25] **ALICE** Collaboration, S. Acharya *et al.*, “Global baryon number conservation encoded in net-proton fluctuations measured in Pb-Pb collisions at $\sqrt{s_{NN}} = 2.76$ TeV”, *Phys. Lett. B* **807** (2020) 135564, arXiv:1910.14396 [nucl-ex].
- [26] V. Vovchenko and V. Koch, “Particlization of an interacting hadron resonance gas with global conservation laws for event-by-event fluctuations in heavy-ion collisions”, *Phys. Rev. C* **103** no. 4, (2021) 044903, arXiv:2012.09954 [hep-ph].
- [27] V. Vovchenko, B. Dönigus, and H. Stoecker, “Canonical statistical model analysis of p-p, p-Pb, and Pb-Pb collisions at energies available at the CERN Large Hadron Collider”, *Phys. Rev. C* **100** no. 5, (2019) 054906, arXiv:1906.03145 [hep-ph].
- [28] T. Neidig, K. Gallmeister, C. Greiner, M. Bleicher, and V. Vovchenko, “Towards solving the puzzle of high temperature light (anti)-nuclei production in ultra-relativistic heavy ion collisions”, *Phys. Lett. B* **827** (2022) 136891, arXiv:2108.13151 [hep-ph].
- [29] A. Andronic, P. Braun-Munzinger, B. Friman, P. M. Lo, K. Redlich, and J. Stachel, “The thermal proton yield anomaly in Pb-Pb collisions at the LHC and its resolution”, *Phys. Lett. B* **792** (2019) 304–309, arXiv:1808.03102 [hep-ph].
- [30] J. Cleymans, P. M. Lo, K. Redlich, and N. Sharma, “Multiplicity dependence of (multi)strange baryons in the canonical ensemble with phase shift corrections”, *Phys. Rev. C* **103** no. 1, (2021) 014904, arXiv:2009.04844 [hep-ph].